









Twitching and Swimming Motility Play a Role in *Ralstonia solanacearum* Pathogenicity

 Jordi Corral,^a  Pau Sebastià,^b  Núria S. Coll,^b  Jordi Barbé,^a  Jesús Aranda,^a  Marc Valls^{b,c}

^aDepartament de Genètica i Microbiologia, Facultat de Biociències, Universitat Autònoma de Barcelona, Cerdanyola del Vallès (Barcelona), Catalonia, Spain

^bCentre for Research in Agricultural Genomics (CSIC-IRTA-UAB-UB), Cerdanyola del Vallès (Barcelona), Catalonia, Spain

^cGenetics Section, Universitat de Barcelona, Barcelona, Catalonia, Spain

Jesús Aranda and Marc Valls contributed equally to this article as senior authors. Author order was determined on the basis of seniority.

ABSTRACT *Ralstonia solanacearum* is a bacterial plant pathogen causing important economic losses worldwide. In addition to the polar flagella responsible for swimming motility, this pathogen produces type IV pili (TFP) that govern twitching motility, a flagellum-independent movement on solid surfaces. The implication of chemotaxis in plant colonization, through the control flagellar rotation by the proteins CheW and CheA, has been previously reported in *R. solanacearum*. In this work, we have identified in this bacterium homologues of the *Pseudomonas aeruginosa* *pil* and *chpA* genes, suggested to play roles in TFP-associated motility analogous to those played by the *cheW* and *cheA* genes, respectively. We demonstrate that *R. solanacearum* strains with a deletion of the *pil* or the *chpA* coding region show normal swimming and chemotaxis but altered biofilm formation and reduced twitching motility, transformation efficiency, and root attachment. Furthermore, these mutants displayed wild-type growth *in planta* and impaired virulence on tomato plants after soil-drench inoculations but not when directly applied to the xylem. Comparison with deletion mutants for *pilA* and *fliC*—encoding the major pilin and flagellin subunits, respectively—showed that both twitching and swimming are required for plant colonization and full virulence. This work proves for the first time the functionality of a pilus-mediated pathway encoded by *pil-chp* genes in *R. solanacearum*, demonstrating that *pil* and *chpA* genes are bona fide motility regulators controlling twitching motility and its three related phenotypes: virulence, natural transformation, and biofilm formation.

IMPORTANCE Twitching and swimming are two bacterial movements governed by pili and flagella. The present work identifies for the first time in the Gram-negative plant pathogen *Ralstonia solanacearum* a pilus-mediated chemotaxis pathway analogous to that governing flagellum-mediated chemotaxis. We show that regulatory genes in this pathway control all of the phenotypes related to pili, including twitching motility, natural transformation, and biofilm formation, and are also directly implicated in virulence, mainly during the first steps of the plant infection. Our results show that pili have a higher impact than flagella on the interaction of *R. solanacearum* with tomato plants and reveal new types of cross-talk between the swimming and twitching motility phenotypes: enhanced swimming in bacteria lacking pili and a role for the flagellum in root attachment.

KEYWORDS *Ralstonia solanacearum*, *pil*, *chpA*, *pilA*, *fliC*

Ralstonia solanacearum is a soilborne Gram-negative bacterium that causes a plant disease known as bacterial wilt mainly in tropical and subtropical climates (1). *R. solanacearum* exhibits an unusually broad host range comprising more than 200 plant

Citation Corral J, Sebastià P, Coll NS, Barbé J, Aranda J, Valls M. 2020. Twitching and swimming motility play a role in *Ralstonia solanacearum* pathogenicity. *mSphere* 5: e00740-19. <https://doi.org/10.1128/mSphere.00740-19>.

Editor Grant R. Bowman, University of Wyoming

Copyright © 2020 Corral et al. This is an open-access article distributed under the terms of the [Creative Commons Attribution 4.0 International license](https://creativecommons.org/licenses/by/4.0/).

Address correspondence to Marc Valls, marcvalls@ub.edu.

Received 14 October 2019

Accepted 19 February 2020

Published 4 March 2020

species from over 50 families, including potato, tomato, tobacco, peanut, and banana, among other crops (2). These facts have contributed to the ranking of *R. solanacearum* as among of the most destructive plant-pathogenic bacterial species worldwide (3).

Plant colonization begins with the attachment of *R. solanacearum* on roots and entry into the host plant through wounds, at sites of secondary root emergence or elongation (4). The bacterium subsequently colonizes the root cortex and moves to the xylem, where it spreads systematically, grows extensively, and produces large amounts of exopolysaccharides (EPS) that cause vascular obstruction. This blockage results in wilting of the stem and leaves and, eventually, plant death (1).

In order to reach different plant tissues and get inside the vascular system, *R. solanacearum* uses different types of movement strategies. The first is swimming motility, an individual cell movement powered by rotating flagella and produced in aqueous environments. In *R. solanacearum*, this kind of motility is mediated by one to four polar flagella and mutants lacking either *FliC* (the flagellar subunit protein) or *FliM* (the flagellar motor switch protein) are nonmotile and present a reduction of virulence in tomato after soil-soak inoculation (5). Chemotaxis enables bacterial cells to sense specific chemicals and depends on the presence of several proteins, which ultimately interact with the flagellar motor to move toward more-favorable conditions. This complex behavior begins in cell membrane-associated receptors, called MCPs (methyl-accepting chemotaxis proteins), which detect environmental stimuli and respond to them by changing their conformation. These changes trigger autophosphorylation of the cytoplasmic histidine autokinase CheA, which forms a complex with the receptor through the coupling protein CheW (Fig. 1A). CheA transfers its phosphate group to CheY, a diffusible cytoplasmic response regulator that interacts with the flagellar motor to switch its direction of rotation. Both *R. solanacearum cheA* and *cheW* null mutants are motile but nonchemotactic, and their virulence is as low as that of a completely nonmotile *fliC* knockout mutant (6).

The other movement used by *R. solanacearum* is twitching motility, a coordinated multicellular movement driven by the extension, attachment, and retraction of the type IV pilus (TFP) appendages in solid surfaces or viscous media. In Gram-negative bacteria, the TFP system requires at least 35 *pil* genes for the synthesis, display, and function of polar and retractable TFP (7). *R. solanacearum* also possesses TFP-mediated motility, which plays a role in natural transformation, biofilm formation, and virulence (8). The genes *pilA*, *pilQ*, and *pilT*, whose products are a monomer of the major pilin protein, the secretin involved in the pilus extrusion, and the protein required for pilus retraction, respectively, have been identified in *R. solanacearum*, and inactivation of any of them reduces both twitching motility and virulence (8, 9). In addition, the *pilA* mutant was reduced in virulence on tomato plants, in attachment to roots, and in biofilm formation as well as being not naturally competent for transformation (8).

In the Gram-negative nosocomial pathogen *Pseudomonas aeruginosa*, which bears both flagella and pili, a hypothetical pilus-mediated chemotaxis pathway encoded by the *pil-chp* genes in so-called cluster IV has been proposed to exist based on homology to the flagellar chemotaxis system (10, 11). In a manner analogous to that seen with flagellum-mediated chemotaxis, in this pathway the molecular signal generated by the cell membrane-associated receptor (PilJ) is expected to trigger autophosphorylation of the cytoplasmic CheA-like histidine autokinase called ChpA, which may form a complex with two CheW homologues called Pill and ChpC (Fig. 1A). The control of movement of pili in this hypothetical system in *P. aeruginosa* is likely performed by two CheY homologues (PilG and PilH), which would interact with the putative TFP motor to control twitching motility after their phosphorylation by ChpA (10, 11).

In this report, we describe a new gene cluster in *R. solanacearum* with strong similarities to *P. aeruginosa* cluster IV, including genes encoding Pill and ChpA homologues. We have constructed *pill* and *chpA* knockout mutants and mutants in well-described twitching (*pilA*) and swimming (*fliC*) motility genes in *R. solanacearum* and have studied the role of these genes in *R. solanacearum* motility and plant colonization

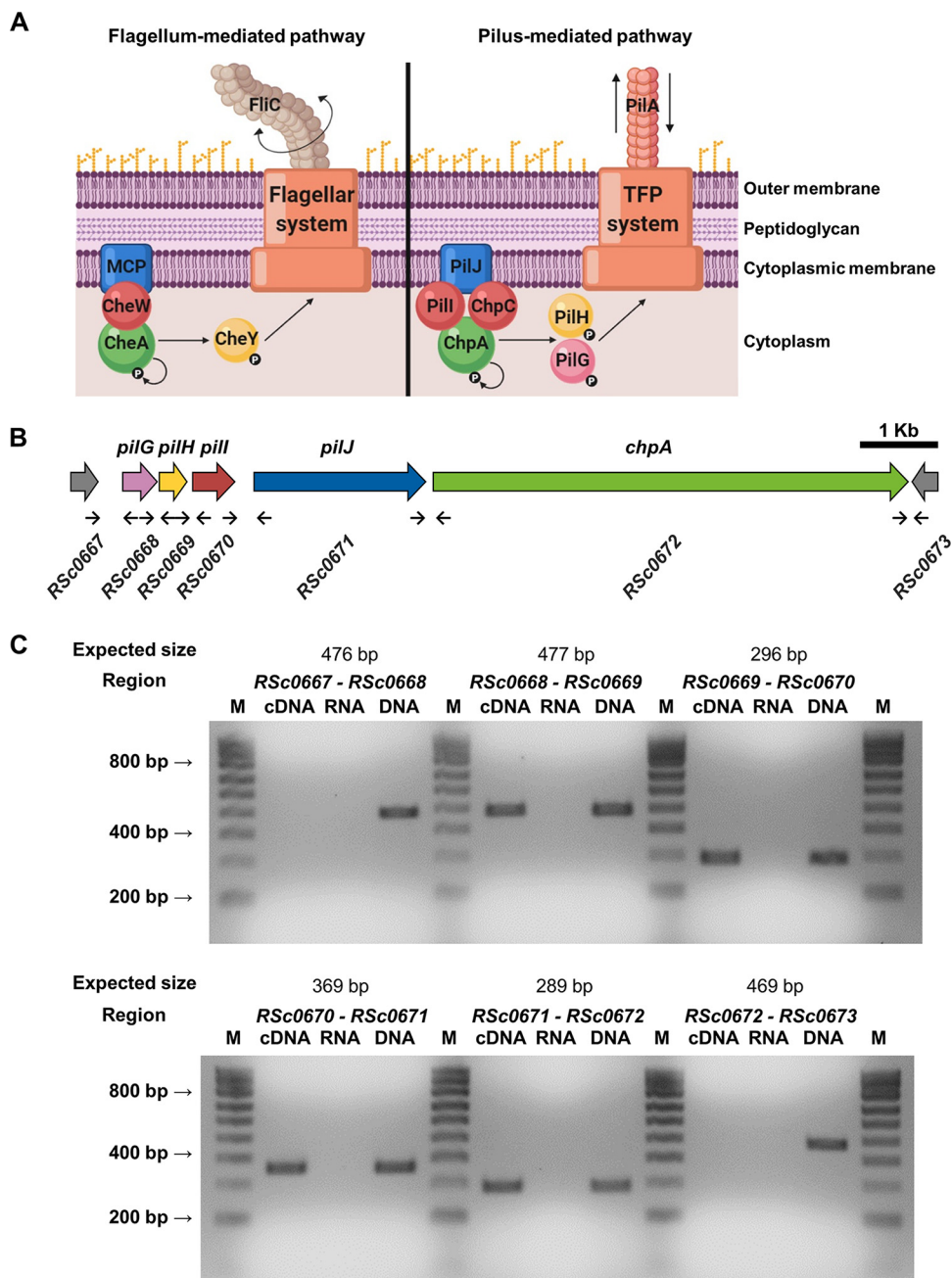


FIG 1 Characterization of the *pil-chp* operon. (A) Representation of flagellin-dependent (left) and pilus-dependent (right) pathways based on protein homology data from Sampedro et al. (11). (B) Schematic diagram of the *pil-chp* operon gene cluster in the *R. solanacearum* GMI1000 genome. Small arrows represent the oligonucleotides used in the RT-PCR. Spacings between protein-coding sequences in the *pil-chp* operon are as follows: *pilG-pilH* 31 bp, *pilH-pill* 58 bp, *pill-pilJ* 245 bp, *pilJ-chpA* 79 bp. (C) RT-PCRs of the indicated *pil-chp* intergenic regions. Each primer pair (Table S1) was used to prepare a PCR mixture with cDNA, RNA, or DNA from the GMI1000 strain as a template. V Ladder NzyTech was used as the DNA marker (M).

and in other related processes such as chemotaxis, biofilm formation, and natural transformation.

RESULTS

Analysis of the *R. solanacearum* GMI1000 genome reveals the presence of single *pill* (CheW-like) and *chpA* (CheA-like) orthologues clustered in a *pil-chp* operon. Orthologous analysis revealed that both TFP-associated protein domains, the CheW-like and CheA-like domains, were found in two genes located in a putative

operon in the GMI1000 genome sequence, which includes in total five *pil-chp* homologues: *R. solanacearum* RSc0668 (*pilG*), RSc0669 (*pilH*), RSc0670 (*pilI*), RSc0671 (*pilJ*), and RSc0672 (*chpA*) (Fig. 1B). This cluster is syntenic to that previously described in *P. aeruginosa*, except that it lacks the *chpB* and *chpC* genes downstream of *chpA*. CheW-like and CheA-like domains were found in the *pilI* and *chpA* genes, respectively, whereas no other CheW-like homologues—such as the mentioned orthologue of *P. aeruginosa* *chpC*—were found in the *R. solanacearum* GMI1000 genome. Compared to its *P. aeruginosa* counterpart (PAO1 protein WP_003084590), the *R. solanacearum* *PilI* homologue presents an identity level of 68%, with fragment coverage of 31%, whereas the *R. solanacearum* *ChpA* homologue shows an identity level of 39.73% with 33.33% coverage with respect to the *P. aeruginosa* *ChpA* (WP_003114893) protein. To determine whether the five *pil-chp* genes are part of the same transcriptional unit, reverse transcription-PCRs (RT-PCRs) were performed (Fig. 1C). The resulting bands confirmed that the *pil-chp* gene cluster is transcribed as a single polycistronic unit, transcriptionally independent of the surrounding RSc0667 and RSc0673 genes (Fig. 1C), predicted to encode a rubredoxin protein and a hypothetical protein, respectively.

The *R. solanacearum* *PilI* and *ChpA* proteins are involved in twitching but not in swimming motility or chemotaxis. To determine the role of *pilI* and *chpA* in *R. solanacearum* motility and chemotaxis, we created null mutants by replacing their protein-coding sequences with a kanamycin cassette. Strains with an inactivated *pilA*, *fliC*, or *cheA* gene were also constructed to be used as controls: the *pilA* mutant was described previously as impaired in twitching (8), the *fliC* mutant as deficient in swimming (5), and the *cheA* mutant as nonchemotactic (6). All mutants obtained were confirmed by PCR (see Fig. S1 in the supplemental material) and subsequent sequencing (Macrogen) using specific primers (see Table S1 in the supplemental material). Furthermore, none of the constructed knockout mutants exhibited macroscopic changes in colonial shape, EPS production (Fig. S2), or growth rate *in vitro* (Fig. S3).

After growth in the appropriate solid medium, colonies of the wild-type (WT) *R. solanacearum* GMI1000 strain exhibited a normal twitching phenotype characterized by irregular colony edges with multiple projections easily observed under light microscopy (Fig. 2A). In contrast, the *pilI* mutant presented round-shaped colony margins without projections, a phenotype identical to that of the nontwitching motility control *pilA* mutant (Fig. 2A). The *chpA* mutant strain also showed impaired twitching movement, but unlike the *pilI* and *pilA* mutants, the reduced twitching motility in the *chpA* mutant was characterized by smaller projections in the colony margins, indicating some residual movement (Fig. 2A). As expected, the *fliC* flagellum mutant control strain presented a twitching phenotype similar to that of the WT GMI1000 strain (Fig. 2A). It is worth noting that the complementation of the *pilI* mutant restored twitching motility, discarding polar effects on downstream genes caused by the *pilI* disruption or by secondary mutations (Fig. S4A).

It was reported previously that inactivation of TFP genes might modify the motility controlled by flagella and vice versa (12–14). Thus, we analyzed the swimming capacity in *pilI* and *chpA* mutants, including again as controls the *pilA* and the *fliC* knockouts, known to be affected only in twitching and swimming motility, respectively (5, 8). After growth in the appropriate semisolid medium, the *pilI* and *chpA* mutants exhibited a typical swimming halo around the inoculated area, similar to that of the WT strain, whereas the *fliC* control mutant was completely impaired in this type of motility, as expected (Fig. 2B). Surprisingly, the *pilA* mutant strain displayed an increased swimming halo compared to that of the WT parental strain (Fig. 2B). Bacterial swimming was more accurately quantified by measuring the dispersion halo at 72 h (Fig. 2C). Significant ($P < 0.05$) differences—more remarkable over time—between the *pilA* mutant and the rest of strains (the WT strain and the *pilI* and *chpA* mutants) showing a normal swimming phenotype were recorded (Fig. 2C). As previously described, the *fliC* control strain showed a significantly reduced swimming halo (Fig. 2C).

In order to determine whether these motility patterns affected bacterial chemotaxis, capillarity assays were performed using Casamino Acids as a chemoattractant (6). Since

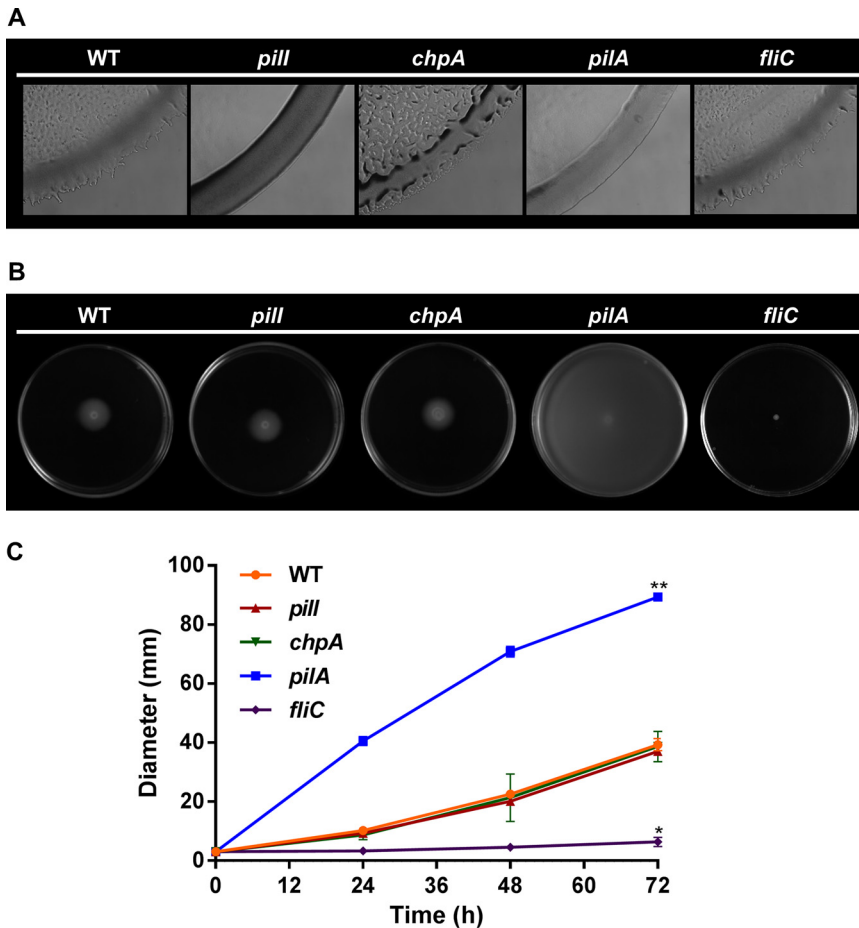


FIG 2 Motility assays. (A) Representative optical microscope images ($\times 100$ magnification) of three independent twitching motility assays. (B) Representative images of three independent swimming motility assays. (C) Representation of the swimming halo diameters measured in three independent assays with three replicates each. Error bars represent standard deviations of the means, and significant ($P < 0.05$) differences from the *R. solanacearum* WT strain are represented as single or double asterisks for a bacterial halo of smaller or larger diameter, respectively.

the *fliC* mutant lacked swimming motility, a *cheA* mutant strain—whose chemotactic response was abolished (6)—was constructed and included in the assays as a more appropriate control. In the parental strain and TFP-related mutants, an approximately 20-fold increase in bacterial counts was observed in capillaries filled with Casamino Acids relative to those containing only chemotaxis buffer (Fig. 3). Thus, with the exception of the motile but nonchemotactic *cheA* knockout, no significant differences in chemotaxis were observed in any TFP-related knockout compared to the WT strain (Fig. 3).

The *R. solanacearum* *pill* and *chpA* mutants present reduced natural transformation abilities. The TFP are essential for bacteria to carry out natural transformation (8). Thus, in order to examine their natural transformation abilities, the WT strain and the corresponding *pill*, *chpA*, *pilA*, and *fliC* knockout mutant counterparts were exposed to DNA containing a gentamicin cassette flanked by ~ 1 -kb-long sequences homologous to a noncoding region of the *R. solanacearum* genome (15) and the frequencies of recovery of gentamicin-resistant colonies were calculated. The results obtained showed that the transformation frequencies of the *pill* and *chpA* mutants were reduced by approximately 20-fold and 6-fold, respectively, compared to the WT strain (Table 1). As expected, the *pilA* mutant, which lacks TFP, was totally unable to take up DNA naturally (8), whereas the *fliC* mutant was transformed with a level of efficiency comparable to that of the WT strain (Table 1).

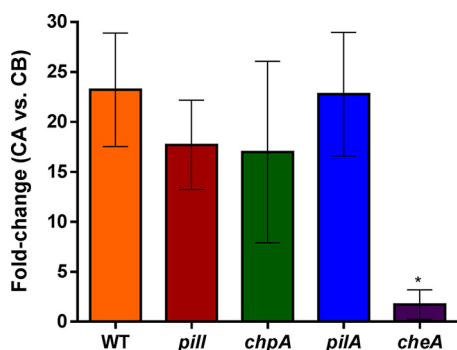


FIG 3 Chemotaxis capillarity assays. Data represent fold change (CFU) between viable bacteria counted in capillaries containing chemoattractant CA (Casamino Acids) divided by the CFU counted in control capillary CB (chemotaxis buffer). Error bars represent standard deviations of the means of results from five replicates per strain, and the asterisk denotes a significant ($P < 0.05$) difference from the *R. solanacearum* WT strain. The assay was performed three times. The results of a representative experiment are shown.

TFP- and flagellin-associated genes are involved in biofilm formation and attachment of *R. solanacearum* to plant roots. Alongside roles in motility, TFP and flagella are required for biofilm formation and initial bacterial adsorption to plant roots (16). We thus measured the capacity of our bacterial mutants to produce biofilm in polystyrene microplate cultures. The *pilA* control mutant was previously shown to produce less-developed biofilms than a WT strain (8), which was quantified here as a significant ($P < 0.05$) reduction ($\sim 70\%$) in biofilm formation. The *chpA* and *fliC* mutants also displayed comparable $\sim 70\%$ reductions in their ability to produce biofilm compared to the GMI1000 strain (Fig. 4A). Interestingly, the *pill* mutant, which exhibited an abolishment of twitching motility similar to that shown by the nonmotile *pilA* mutant, presented a significant ($P < 0.05$) increase of $\sim 25\%$ in biofilm formation with respect to the WT parental strain (Fig. 4A). Furthermore, the complemented *pill* mutant showed a restored ability to produce biofilm (Fig. S4B).

Next, we incubated each bacterial strain with isolated tomato roots and quantified their capacity to attach to the root surface. The results of these experiments showed that all TFP mutants (*pill*, *chpA*, and *pilA*) presented a statistically significant ($P < 0.05$) 10-fold-lower level of root attachment than the WT GMI1000 strain (Fig. 4B). Furthermore, the aflagellated *fliC* mutant also displayed a statistically significant ($P < 0.05$) 5-fold decrease compared with the WT strain (Fig. 4B), denoting that both TFP and flagella promote adhesion between *R. solanacearum* cells and tomato roots.

The *pill* and *chpA* mutants show reduced virulence in soil-soak inoculations but not when directly inoculated in the stem of tomato plants. To determine the effect of Pill and ChpA on *R. solanacearum* pathogenicity, tomato plants were infected by drenching the soil with the collected bacterial solution without wounding the roots, which mimics the natural infection process of this soilborne pathogen. The four mutants analyzed (*pill*, *chpA*, *pilA*, and *fliC*) exhibited a significant ($P < 0.05$) reduction in their ability to develop plant wilting compared to the parental WT strain, but to

TABLE 1 Natural transformation frequencies of the indicated *R. solanacearum* strains^a

Strain	Natural transformation frequency ^b
GMI1000 WT	$1.05 (\pm 1.2) \times 10^{-6}$
<i>pill</i>	$5.07 (\pm 4.9) \times 10^{-8}$
<i>chpA</i>	$1.78 (\pm 1.5) \times 10^{-7}$
<i>pilA</i>	$< 2.57 \times 10^{-9}$
<i>fliC</i>	$1.66 (\pm 2.1) \times 10^{-6}$

^aEach experiment was carried out in triplicate in five independent assays.

^bNatural transformation frequency data are represented as means \pm standard deviations and were calculated as the number of recombinant colonies by the total number of viable cells. At least 10% of the recombinant colonies obtained for each strain were confirmed by sequencing.

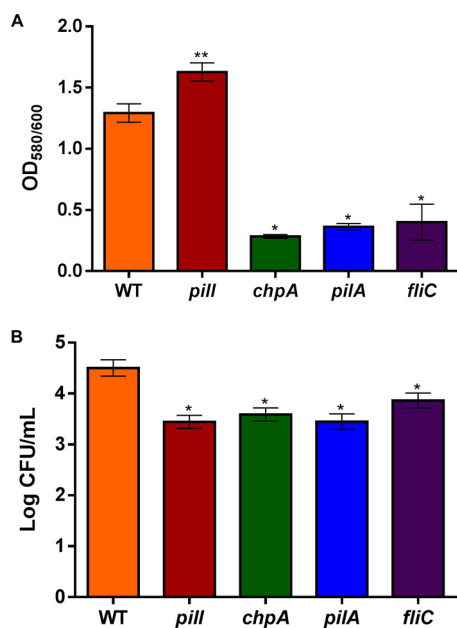


FIG 4 Biofilm and root attachment quantification. (A) Biofilm assay in which y-axis data represent biofilm absorbance (OD₅₈₀) divided by the biomass (OD₆₀₀). The error bars represent standard deviations of the means of results from 16 replicates per strain. Significant ($P < 0.05$) differences from the *R. solanacearum* WT strain are represented as single or double asterisks for lower or higher absorbance ratio values, respectively. The assay was performed three times. The results of a representative experiment are shown. (B) Representative root attachment assay showing means of logarithms of counts of viable bacteria (CFU). Error bars represent standard errors of the means of data from five 1-week-old tomato roots per assay, and asterisks denote significant ($P < 0.05$) differences from the *R. solanacearum* WT strain. The assay was performed three times. The results of a representative experiment are shown.

differing degrees (Fig. 5A). Statistical analysis classified the mutants into four groups: the *pilA* deletion mutant was the least virulent, followed by the *pill* and *chpA* mutants, with both showing an intermediate phenotype, and the *fliC* mutant, with a small but significant decrease in apparent wilting compared to the WT parental strain (Fig. 5A). Bacterial counts obtained from 3-cm stem cuts from tomato plants infected using the same procedure were also carried out at 4, 8, and 12 dpi (days postinoculation). Only the *pilA* mutant exhibited a significant (2 log) reduction at days 4 and 12 ($P < 0.05$) with respect to the rest of strains, whose numbers in stem tissues were similar to those seen with the WT strain (Fig. 5B). To discard any potential fitness effects resulting from the growth of the knockout strains in tomato plants, all strains were infiltrated in tomato leaves. The results showed no differences in bacterial growth of any of the mutants with respect to the WT (Fig. 5C). In contrast, when tomato plants were infected by direct petiole injection, *pill* and *chpA* knockout strains showed no statistically significant reduction in their capacity to wilt plants (Fig. 6A), while the control *pilA* mutant exhibited significant ($P < 0.05$) differences in disease index in comparison to the WT, as previously described (8). Finally, the virulence of the flagellum-deficient *fliC* mutant was also comparable to that of the WT strain (Fig. 6A). Bacterial counts measured over time in infected plant stems were similar to those reached by the WT strain for all mutants except for the *pilA* mutant, which presented a significant ($P < 0.05$) reduction in plant colonization (Fig. 6B). Interestingly, the *fliC* mutant exhibited a reduction in stem numbers only at 3 dpi, reaching values similar to those shown in the *pill* and *chpA* mutants and the WT strains at later infection times (Fig. 6B).

Deletion of *pilA* but not *pill*, *chpA*, and *fliC* limits bacterial spread in plant tissues. In order to study the distribution of *pill*, *chpA*, *pilA*, and *fliC* *R. solanacearum* knockout mutants along tomato plants, reporter strains were constructed through the insertion into their genome of the *luxCDABE* operon under the control of the *hrpB* promoter (Fig. 5G). Tomato plants grown in pots were soil-inoculated with the reporter

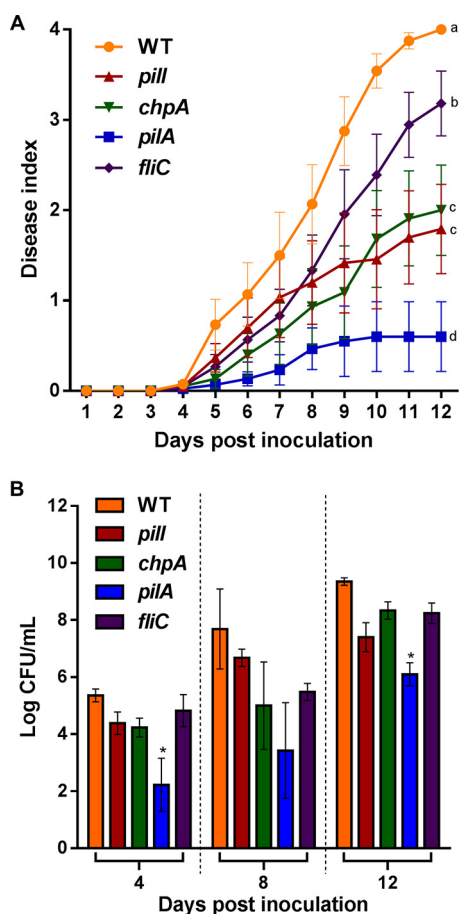


FIG 5 Drenching assays. (A) Disease index scaled from 0 (no wilt) to 4 (death), with levels measured daily after soil soaking of 4-week-old tomato plants by the use of a naturalistic inoculation method. Error bars represent standard errors of the means of results from 20 replicates per strain. According to their wilting reduction ($P < 0.05$), strains are classified in four groups (labeled a through d). The assay was performed three times. The results of a representative experiment are shown. (B) Logarithm of counts of viable bacteria (CFU per milliliter) after soil soaking of 4-week-old tomato plants by the use of a naturalistic soil soak inoculation method at 4, 8, and 12 days postinoculation. Error bars represent standard errors of the means of results from 20 replicates per strain. Asterisks denote significant ($P < 0.05$) differences from the *R. solanacearum* WT strain. The assay was performed three times. The results of a representative experiment are shown.

strains, and luminescence in different stem sections was recorded at 3 and 6 dpi. At 3 dpi, no significant differences were observed between any of the knockouts and the WT strain at any stem height (Fig. 7). However, at 6 dpi, the *pilA* mutant carrying the *luxCDABE* operon exhibited a significant ($P < 0.05$) reduction of its luminescence compared to the WT reporter strain (Fig. 7). No significant differences in colonization between the stem sections from internodes 2 and 3 were observed for any other strain at 6 dpi (Fig. 7). To confirm that expression of the reporter operon was not affected by any of the gene disruptions, bacterial growth and luminescence were both measured over time in *in vitro* cultures (Fig. S7). In these experiments, all mutants showed comparable levels of luminescence and indistinguishable differences in growth from the WT strain, ruling out an inhibition of the reporter in the *PilA* mutant (Fig. S7).

DISCUSSION

A conserved cluster involved in twitching motility. In this study, we identified a new gene cluster in *R. solanacearum* strain GM11000 (Fig. 1B) presenting synteny with respect to *P. aeruginosa* and *Lysobacter enzymogenes* cluster IV (17–19) and the *Xylella fastidiosa pil-chp* operon (20). With the construction of pilus- and ChpA-deficient strains, we demonstrated the involvement of these genes in *R. solanacearum* twitching but not

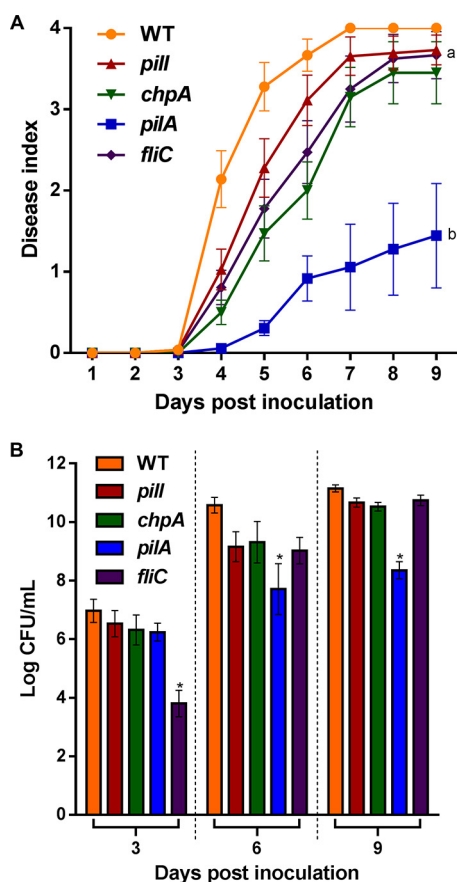


FIG 6 Petiole inoculation assays. (A) Disease index scaled from 0 (no wilt) to 4 (death), measured daily in 4-week-old tomato plants after the use of a direct inoculation method. Error bars represent standard errors of the means of results from 20 replicates per strain. According to statistically significant differences ($P < 0.05$), strains were classified in two groups (labeled a and b). The assay was performed three times. The results of a representative experiment are shown. (B) Logarithms of viable bacteria (CFU per milliliter) of the indicated *R. solanacearum* strains counted by the use of a direct inoculation method using 4-week-old tomato plants at 3, 6, and 9 dpi. Error bars represent standard errors of the means of results from 20 replicates per strain, and asterisks denote significant ($P < 0.05$) differences from the *R. solanacearum* WT strain. The assay was performed three times. The results of a representative experiment are shown.

in swimming (Fig. 2). Whereas the *chpA* mutant presented reduced twitching, *Pill* inactivation produced a total abolition of this movement, comparable to that seen with the nontwitching *pilA* control (Fig. 2A). Decreased twitching motility has been similarly observed in *chpA* (CheA-like) knockout mutants in other bacteria such as *P. aeruginosa* (21) and *X. fastidiosa* (20) and in the *pill* (CheW-like) null mutant of *P. aeruginosa* (22). However, the *pill* knockout remains twitching proficient in *L. enzymogenes* (23), indicating differences in TFP gene function that depend on the bacterial species. In contrast to our results seen in *R. solanacearum* revealing that the *chpA* mutant showed some residual twitching motility, both *pill* and *chpA/pilL* mutants in *Acidovorax citrulli* lacked twitching motility and did not produce TFP (24). However, a *pilJ* mutant in the *A. citrulli pil-chp* operon retained the ability to produce TFP (13).

TFP influence swimming motility. Since the inactivation of specific genes associated with one type of appendage may affect the movement controlled by others (12–14, 25), swimming motility assays were also performed with the *R. solanacearum* mutants that had been constructed. Surprisingly, results obtained showed swimming hypermotility performed by the *pilA* mutant (Fig. 2B and C), a phenomenon observed in other *R. solanacearum* knockouts such as those lacking the transcriptional regulators *phcA* (26) and *motN* (27), the latter being chemotaxis proficient like the *R. solanacearum*

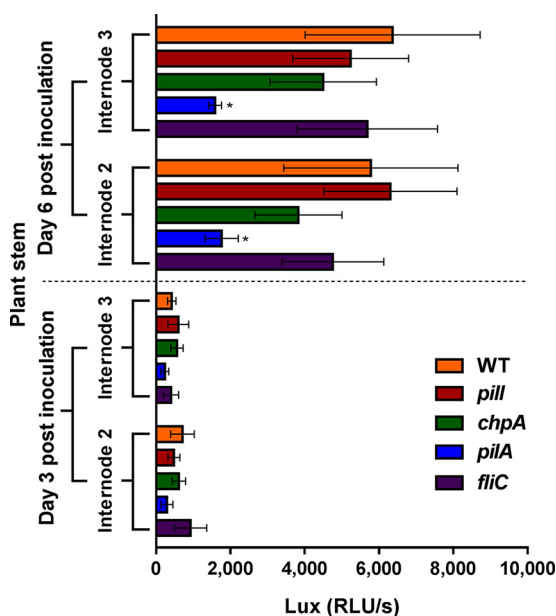


FIG 7 Bacterial spread in plant tissue. Luminescence detection of the indicated *R. solanacearum* strains prepared by the use of a direct inoculation method was performed using 4-week-old tomato plants at 3 and 6 dpi. x-axis data represent means of luminescence (RLU/s) data from 10 replicates per strain. Error bars represent standard errors of the means, and asterisks denote significant ($P < 0.05$) differences from the *R. solanacearum* WT strain. The assay was performed three times. The results of a representative experiment are shown.

pilA mutant (Fig. 3). Cross-effects between the two appendage-dependent movements are likely underestimated due to the comparative paucity of studies in which both swimming and twitching assays have been carried out to evaluate the effect of single mutants. One example of this connection is found in the PilS-PilR two-component system of *P. aeruginosa*, which regulates TFP expression and whose inactivation also causes a reduction in swimming motility (25). Similarly, the inactivation of genes encoding PilA, the pilus assembly protein PilO, or two predicted minor pilins, FimU and FimT, caused reduced twitching but complete abolition—or, in the case of the *fimT* mutant, impairment—of swimming in *P. syringae*, suggesting that TFP are involved not only in twitching but also in swimming (14).

***R. solanacearum* Pill and ChpA play a role in all known TFP-related functions.**

As previously reported in *R. solanacearum* studies of the *pilA* mutant, TFP are required for natural transformation and biofilm formation (8). Our results demonstrate that Pill and ChpA also contribute to natural competence (Table 1), presumably through proper regulation of TFP. Regarding biofilm formation, our data showed that Pill and ChpA play contrary roles (Fig. 4A). Interestingly, knockouts lacking either PilA or PilQ in *Xanthomonas* spp. displayed reduced twitching motility, but biofilm formation was affected only in the *pilQ* mutant (28, 29). On the other hand, in the *A. citrulli fliR*-null mutant, whose swimming and twitching movements remained impaired, no effect on biofilm development was observed (12). Besides their roles in natural transformation and biofilm formation, TFP are also key for bacterial virulence (7). In *R. solanacearum*, virulence processes during plant colonization have been investigated in some TFP-related genes such as *pilA* (8) and *pilQ* (30), highlighting the relationship between twitching motility and virulence (31–33). Our data demonstrate that Pill and ChpA proteins are required for early pathogenic stages that result in effective plant colonization and wilting. This is shown by the fact that strains deleted of these genes caused reduced wilting in response to a naturalistic infection method (soil drenching; Fig. 5A) but behaved like the WT when applied directly by petiole inoculation, a procedure that overcomes all initial steps of plant colonization until the bacterium reaches the xylem (Fig. 6A). Similarly, our data corroborate the idea that PilA plays a role in the pathogenesis of *R.*

solanacearum, as previously reported (5, 8), because this mutant showed impaired multiplication *in planta* in both root drenching and petiole inoculation experiments (Fig. 5B and 6B) and restricted stem colonization (Fig. 7). Involvement of TFP gene inactivation and virulence has also been described in several bacterial plant pathogens such as *P. syringae* (14), *Xanthomonas* spp. (28, 34), *A. citrulli* (13), and *X. fastidiosa* (20, 35), in which an impairment of twitching motility resulted in the development of a reduced pathogenic phenotype. Remarkably, although all TFP mutants analyzed showed similar phenotypes in biofilm formation, root attachment, and chemotaxis (Fig. 3 and 4), the *pill* and *chpA* deletion mutants showed milder phenotypes than the *pilA* mutant in transformation efficiency and in the various virulence and plant colonization assays performed (Table 1; see also Fig. 5 and 7). This can be explained by the fact that, while PilA is the structural pilus subunit and its mutant is nonpilliated, the Pill and ChpA are regulator proteins in TFP assembly and their deletion mutants may still present some TFP, as indicated by the residual twitching motility displayed by the *chpA* knockout strain (Fig. 2A). In this sense, it is worth mentioning that disruption of the *chpA* homolog gene in *X. fastidiosa* (*pilL*) resulted in a loss of twitching motility but in retention of the ability to produce TFP, resembling the phenotype of the *R. solanacearum chpA* mutant, although in the latter some residual twitching motility was observed, maybe because of differences in the experimental settings.

Novel roles of flagella in *R. solanacearum* GMI1000. This work demonstrates that adhesion to roots via TFP is crucial for optimal plant colonization and disease development but also that flagella are involved in these processes (Fig. 4B). Implication of flagella in attachment to both animal and plant cells has been recently reported in bacterial pathogens at the early stage of infection (36–38). Although flagella have not been reported to play a role in attachment of members of the *Xanthomonadaceae* (39), in other bacterial species such as *Azospirillum brasilense*, flagellin-deficient mutants are impaired in attachment to wheat roots, and the purified polar flagellum binds directly to the wheat root surface (40).

In addition, our results shown that *fliC* inactivation produces a reduction in biofilm formation (Fig. 4A), indicating that flagella also contribute to this process in *R. solanacearum* GMI1000, as had been observed in *P. aeruginosa* and other bacteria (41, 42). In contrast, inactivation of either *fliC* or genes involved in aerotaxis—an active cell movement along oxygen gradients—in *R. solanacearum* strain K60 caused increased biofilm production (43), indicating strain-specific TFP functions.

The flagellar protein FliC was previously shown to play a role in pathogenesis of *R. solanacearum*, especially during the first steps of the interaction (5, 8). Here, we also observed that the *fliC* deletion mutant caused reduced wilting only when inoculated by root drenching and not by direct petiole inoculation (Fig. 5A and 6A). However, this flagellum-deficient mutant was affected only slightly in its capacity to multiply *in planta* (Fig. 6B) and colonize the plant stem (Fig. 7), in contrast with the stronger phenotypes shown by the nonpilliated *pilA* strain. We conclude that TFP are more important than flagella for the interaction of *R. solanacearum* with tomato plants.

Conclusion. In this work, we have demonstrated that the virulence of *R. solanacearum pill*, *chpA*, *pilA*, and *fliC* deletion mutants is impaired in the first stages of plant colonization and that the *pilA* mutant shows decreased growth after drenching or petiole inoculation. This is the first report on the putative *R. solanacearum* type IV pilus regulators Pill and ChpA, where we clearly demonstrate their role in twitching motility, biofilm formation, natural transformation, and virulence. Additionally, a hypermotile swimming phenotype in GMI1000 strain lacking PilA and the role of FliC in root attachment and biofilm formation have been described here for the first time. Our work suggests that further research in *R. solanacearum* should be addressed to elucidate putative connections between swimming and twitching motilities in both well-documented genes and genes with unknown function.

TABLE 2 Bacterial strains and plasmids used in this work^a

Strain or plasmid	Relevant characteristics	Source or reference
Strains		
<i>E. coli</i> DH5 α	<i>E. coli</i> supE4 Δ lacU169 (80 Δ lacZ Δ M15) hsdR17 recA1 endA1 gyrA96 thi-1 relA1	Clontech
<i>R. solanacearum</i> GMI1000	Wild-type strain (phylotype I, race 1 biovar 3)	45
<i>R. solanacearum</i> GMI1000 PhB-lux	GMI1000 strain with <i>PhrpB-lux</i> from pRCGent-PhB-lux, Gm ^r	This work
<i>R. solanacearum</i> pill	GMI1000 strain with Δ pill::loxP-Km from pCM184, Km ^r	This work
<i>R. solanacearum</i> pill PhB-lux	Pill with <i>PhrpB-lux</i> from pRCGent-PhB-lux, Km ^r , Gm ^r	This work
<i>R. solanacearum</i> chpA	GMI1000 strain with Δ chpA::loxP-Km from pCM184, Km ^r	This work
<i>R. solanacearum</i> chpA PhB-lux	ChpA strain with <i>PhrpB-lux</i> from pRCGent-PhB-lux, Km ^r , Gm ^r	This work
<i>R. solanacearum</i> pilA	GMI1000 strain with Δ pilA::loxP-Km from pCM184, Km ^r	This work
<i>R. solanacearum</i> pilA PhB-lux	PilA strain with <i>PhrpB-lux</i> from pRCGent-PhB-lux, Km ^r , Gm ^r	This work
<i>R. solanacearum</i> fliC	GMI1000 strain with Δ fliC::loxP-Km from pCM184, Km ^r	This work
<i>R. solanacearum</i> fliC PhB-lux	FliC strain with <i>PhrpB-lux</i> from pRCGent-PhB-lux, Km ^r , Gm ^r	This work
<i>R. solanacearum</i> cheA	GMI1000 strain with Δ cheA::loxP-Km from pCM184, Km ^r	This work
Plasmids		
pCM184	Allelic exchange vector, carrying kanamycin cassette flanked by <i>loxP</i> , Ap ^r , Km ^r	Addgene
pGEMT	Cloning vector, Ap ^r	Promega
pRCGent-Pps-GWY	Vector carrying gentamicin cassette flanked by regions homologous to the GMI1000 genome, Ap ^r , Gm ^r	15
pRCGent-PhB-lux	Vector carrying <i>luxCDABE</i> operon from pMU1 cloned in KpnI–NotI in pRCGent-PhB, Ap ^r , Gm ^r	49
pBT4	Broad-host-range vector carrying the pBBR1 replicon, Tc ^r	Addgene
pDSK-GFPuv	Vector carrying the <i>PpsbA</i> promoter, Km ^r	LiveScience

^aKm^r, Gm^r, Ap^r, and Tc^r stand for resistance to kanamycin, gentamicin, ampicillin, and tetracycline resistance, respectively.

MATERIALS AND METHODS

Bacterial strains, plasmids, plant material, and growth conditions. The bacterial strains and plasmids used in this study are listed in Table 2. *Escherichia coli* DH5 α was grown at 37°C in Luria-Bertani (LB) (44) agar or in LB broth with shaking at 180 rpm. The *R. solanacearum* GMI1000 WT strain and derivative mutants were routinely grown at 28°C in rich B medium, Boucher's minimal medium (MM) (45), and CPG (Casamino Acids-peptone-glucose) medium (46) agar or broth with shaking at 180 rpm. When necessary, rich B medium was supplemented with 0.5% glucose and 0.005% 2,3,5-triphenyltetrazolium chloride (final concentration) in agar plates, and MM broth was supplemented with 2% glycerol or 20 mM glutamate (final concentration). When needed, ampicillin (50 mg/liter), kanamycin (50 mg/liter), gentamicin (10 mg/liter), or tetracycline (5 mg/liter) was added in growth media. For phytopathogenesis assays, tomato plants (*Solanum lycopersicum* cultivar Marmande) were used to evaluate virulence of *R. solanacearum*. Plants were routinely grown in pots in a mixed soil of Substrate 2 (Klasmann-Deilmann GmbH, Geeste, Germany), perlite, and vermiculite at a proportion of 30:1:1 for 1 to 4 weeks at 22°C and 60% relative humidity under long-day light regimen conditions (16 h light and 8 h darkness). Before the infectious assays, tomato plants were acclimated at least 3 days by transferring them to a growth chamber at 27°C under the same humidity and photoperiod conditions.

RNA extraction and RT-PCR. Total RNA was extracted by the use of an RNeasy minikit (Qiagen, Hilden, Germany) from 5-ml cultures at an absorbance level of 0.4 (optical density at 600 nm [OD₆₀₀]) that had previously been pelleted and treated with lysozyme (50 mg/ml) and resuspended in Tris-EDTA (TE) buffer for 10 min at 37°C. Once extracted, the RNA was incubated with DNase Turbo Ambion (Thermo Fisher, Waltham, MA) to remove DNA contaminants, and PCR analysis of the mixtures performed using RNA samples without reverse transcriptase confirmed the absence. Reverse transcription of RNA was performed through the use of a first-strand cDNA synthesis kit (Nzytech, Lisbon, Portugal) and the appropriate primers (listed in Table S1 in the supplemental material). All molecular techniques were performed using standard procedures.

Gene identification and construction of *R. solanacearum* knockouts and of complemented and reporter strains. The *P. aeruginosa* Pill and ChpA homologues in *R. solanacearum* were identified through mapping coded proteins to nonsupervised orthologous groups (NOGs) using the eggNOG v4.0 Web service (47) and complete *R. solanacearum* GMI1000 chromosome (NC_003295.1) and megaplasmid (NC_003296.1) sequences. Knockout deletion mutants *pill* (WP_011000625), *chpA* (WP_011000627), *pilA* (WP_011000517), *fliC* (WP_011003694), and *cheA* (WP_011004658) were generated by replacing the coding sequence of each target gene by a kanamycin resistance cassette as described previously (48). To this end, DNA fragments corresponding to ~1 kb of the upstream and downstream flanking regions of each gene and a kanamycin cassette flanked with *loxP* regions were PCR amplified from the *R. solanacearum* GMI1000 genome and plasmid pCM184 (Addgene), respectively. The oligonucleotides used (Table S1) included overlapping regions enabling the three fragments to be fused in two amplification rounds. All PCRs were performed using proofreading Phusion High-Fidelity DNA polymerase (Thermo Fisher). Next, 3' A overhangs were added to the final PCR products using *Taq* polymerase (Invitrogen, Waltham, MA) and the fragments were cloned into pGEM-T plasmid (Promega, Madison, Wisconsin), transformed in *E. coli* DH5 α , and selected in ampicillin- and kanamycin-containing LB plates.

Sequenced constructs (Macrogen, Seoul, South Korea) were amplified with appropriate primers (Table S1), and the final product was purified (NZYGelpure; Nzytech), naturally transformed in *R. solanacearum* strain GM11000, and plated in kanamycin B rich medium for mutant selection (49). For complementation, the *PpsbA* promoter and the corresponding gene were amplified from the pDSK-GFPuv (LifeScience) plasmid and the *R. solanacearum* GM11000 genome, respectively. Then, both fragments were cloned into the pBT4 vector (Addgene) using Gibson assembly master mix (New England Biolabs, Ipswich, Suffolk, United Kingdom) and the appropriate primers (Table S1). Knockouts were then electroporated with the constructed plasmid and selected in tetracycline-containing medium plates. To construct luminescent reporter strains, integration of the *luxCDABE* operon under the *hrpB* promoter was carried out as previously described (49). Briefly, the reported operon was amplified from the pRCGent-PhB-lux plasmid using the appropriate primers and electroporated to each strain. Transformants were selected on gentamicin-containing B rich plates. All knockouts and reported strain verifications were carried out by PCR amplification and sequencing (Macrogen) with the corresponding primers indicated in Table S1.

Twitching and swimming assays. Modified CPG plates with 0.3% and 1.6% Difco agar were used on the day of their preparation for analysis of swimming and twitching motilities, respectively (50). Both motility tests were carried out by the inoculation of a 2- μ l drop of a bacterial suspension into Mill-Q (MQ) water at an absorbance level of 0.1 (OD_{600}) in the middle of the appropriate plate. After inoculation, both CPG-type plates were incubated at 30°C and 24 h for twitching (until layered edges with multiple irregular projections were observed in the WT strain) and 72 h for swimming (measuring the bacterial halo daily). A Zeiss Axiomager M2 microscope (Carl Zeiss Microscopy, Oberkochen, Germany) was used to obtain representative images of twitching motility at 40 \times increases. A ChemiDoc XRS+ system (Bio-Rad, Hercules, CA) was used to obtain swimming motility images.

Chemotaxis capillary assays. To establish chemotactic effects in *R. solanacearum* knockouts, capillary assays were carried out as described previously (51), with some modifications. Briefly, three V-shaped bent needles (Nipro; Kita-ku, Osaka, Japan) covered with a 24-by-65 mm microscope coverslip (Menzel-Glasser; VWR, Radnor, PA) were placed on the surface of aseptic 140-mm-diameter petri dishes (Deltalab; Rubi, Barcelona, Spain) to form the chemotaxis chambers. Sealed and autoclaved 1-ml capillaries (Microcaps, Drummond Scientific Co., Broomall, PA) (3 cm in length) were filled with chemotactic buffer (CB) as a negative control or with CB with 2% Casamino Acids as a chemoattractant (6). Bacterial suspensions were prepared from overnight cultures in B rich medium with the appropriate antibiotics, washed twice with MQ water, and adjusted to an OD_{600} of 0.1. Chemotaxis chambers were filled with the corresponding bacterial suspensions and incubated at 30°C during 2 h. Once incubated, the capillaries were washed twice to remove any external attached cell and then broken off, and the content was poured into a microcentrifuge tube containing 1 ml of MQ water. Proper dilutions were plated in rich B medium, and the CFU counts per milliliter obtained under each set of conditions were normalized between the capillaries treated with 2% Casamino Acids and those left untreated.

Natural transformation assays. Natural transformation efficiencies were determined as previously described (52). Briefly, 100 ng of DNA containing a gentamicin cassette with homologous regions amplified from pRCG-Pps-GWY (53) was added to each 50- μ l volume of the corresponding strains grown in MM broth supplemented with 2% glycerol. Transformed clones were selected on gentamicin-containing B rich medium plates and verified by PCR and sequencing (Macrogen) with the corresponding primers indicated in Table S1. The same cultures were also plated in B rich medium without antibiotic to obtain the total number of viable bacteria (CFU per milliliter). Transformation frequencies were calculated as the number of recombinant colonies divided by the total number of CFU per milliliter.

Biofilm quantification. Quantitative analysis of *R. solanacearum* biofilm formation was carried out through crystal violet assay by the use of a method adapted from previous work (54). Briefly, CPG overnight cultures were collected, washed, and adjusted in CPG to an OD_{600} of 0.1. Next, 95 μ l of CPG broth and 5 μ l of each bacterial suspension were added onto 96-well polystyrene microplates (Greiner, Kremsmunster, Austria) and incubated without shaking at 30°C during 24 h. After incubation, biomass growth in wells was measured at an OD_{600} . Subsequently, wells were washed twice with MQ water, incubated with 100 μ l of 0.1% crystal violet stain, and incubated at room temperature for 30 min. Wells were then washed with MQ water three times, and the stained biofilm immobilized on the wells was solubilized with 100 μ l of 95% ethanol and measured at OD_{580} . Measurements were performed using a multiplate reader (Sunrise, Tecan, Zurich, Switzerland), and results were normalized according to previously obtained biomass absorbance (OD_{580}/OD_{600}).

Root attachment quantification. Attachment to tomato roots was carried out as previously described (55), with slight modifications. One- or 2-week-old plants, grown as described above without previous acclimation, were collected and washed. Roots were submerged in 1 ml of bacterial culture (approximately 10^6 CFU), obtained from a diluted culture at an OD_{600} of 0.1 ($\sim 10^8$ CFU/ml) in MQ water. Submerged root plants were incubated at 25°C with gentle shaking at 50 rpm during 4 h to promote bacterium-root contact. After incubation, roots were placed in tubes with 30 ml sterile 0.88% NaCl, shaken during 1 min at 200 rpm to remove unattached bacteria, and gently dried to remove liquid excess. Attached bacteria were then collected by immersing 2-cm-long dried roots in tubes with 1 ml sterile 0.88% NaCl, followed by 1 min of vortex mixing. Appropriated dilutions were plated in B rich medium.

Bacterial leaf multiplication assays. Bacterial growth *in planta* was measured as previously described (56), with some modifications. A 3-liter inoculum of each bacterial strain was prepared, starting from a culture maintained at an OD_{600} of 0.1 in MQ water (approximately 10^8 CFU/ml) to obtain a final concentration of $\sim 10^5$ CFU/ml. Infections were performed using a vacuum machine, and to reduce the

surface tension of the water, 150 μ l of Silwet L-77 was added to the 3-liter inoculum. Four-week-old tomato plants were submerged in the respective bacterial inocula, and vacuum was applied during 1 min to promote bacterial infiltration in leaves. After inoculation, plants were retrieved, dried, and incubated under standard conditions (27°C, 60% relative humidity, and 16-h light/8-h darkness). At specific dpi, four 5-mm² leaf disks were recovered from the infiltrated plants, collected in tubes containing 200 μ l of MQ water, and subjected to a grinding process. The collected dilutions were plated on B medium to obtain the final concentration of each strain on leaf surface (expressed as CFU count per square centimeter).

Bacterial virulence experiments. For drenching assays, 4-week-old unwounded plants were soil-soak inoculated by watering with 40 ml of bacterial culture, at an OD₆₀₀ of 0.1 (~10⁸ CFU/ml) in MQ water, per plant (56). Once infected, plants were incubated under standard conditions and wilting signs were recorded daily on a disease index scale from 0 (no wilt) to 4 (death). At 4, 8, and 12 dpi, bacterial multiplication in tomato plants was measured by collecting 3 cm of the stem, 0.5 cm above the petiole of the first true leaf, into tubes containing 300 μ l of MQ water. After 30 min of incubation at room temperature, serial dilutions were plated in corresponding rich B medium to measure viable bacteria.

For petiole inoculation assays, 4-week-old plants were directly infected by inoculation with a 100- μ l drop (approximately 10³ CFU) of a sample obtained from a culture at OD₆₀₀ of 0.1 (~10⁸ CFU/ml) diluted in MQ water. Bacterial injections into the stem, above the petiole of the first true leaf, were performed using a sterile needle, and plants were incubated under standard conditions (56). Disease index scale values were assigned daily during 9 days, and at 3, 6, and 9 dpi, bacterial multiplication in tomato plants was measured as previously described by collection of 3 cm of the stem, 0.5 cm above the inoculation point, and plating in corresponding rich B plates.

Luminescence assays. Overnight cultures of all strains carrying *PhrpB::lux* were inoculated in MM supplemented with glutamate and gentamicin at absorbance of 0.3 (OD₆₀₀), and culture aliquots were collected at 0, 4, 6, and 8 h postinoculation to measure luminescence and absorbance (57). Expression of the *hrpB* promoter was represented as relative light units (RLU) per second. A FB-12 luminometer (Berthold Detection Systems, Pforzheim, Germany) and a V-1200 spectrophotometer (VWR, Radnor, PA) were used for each measurement, respectively.

To evaluate bacterial distribution through plant stem of reporter strains, 4-week-old plants were infected as previously described in a petiole inoculation assay but with slight modifications. Drops (10 μ l) of cultures of each luminescent strain (approximately 10³ CFU) were injected into the plant stem, above the petiole of the second true leaf. Once infected, plants were incubated under standard conditions and at 3 and 6 dpi, luminescence in tomato plants stem was measured by collecting 0.5 cm of internodes 2 and 3 into tubes containing 200 μ l of MQ water. After 30 min of incubation, luminescence was measured from different stem cuts.

Statistics. All data were analyzed in a two-tailed, one-way analysis of variance (ANOVA) followed by the Tukey test for *post hoc* multiple-group comparisons. Results were considered statistically significant when a *P* value of <0.05 was obtained.

Data accessibility. The data that support the findings of this study are available from the corresponding author upon request.

SUPPLEMENTAL MATERIAL

Supplemental material is available online only.

FIG S1, TIF file, 1.3 MB.

FIG S2, TIF file, 2.5 MB.

FIG S3, TIF file, 0.5 MB.

FIG S4, TIF file, 1.5 MB.

FIG S5, TIF file, 0.5 MB.

FIG S6, TIF file, 1.1 MB.

FIG S7, TIF file, 0.5 MB.

TABLE S1, DOCX file, 0.01 MB.

ACKNOWLEDGMENTS

This study was funded by grants BIO2016-77011-R and AGL2016-78002-R (Spanish Ministry of Economy and Competitiveness). We acknowledge financial support from the Severo Ochoa Program for Centers of Excellence in R&D (SEV-2015-0533) and the CERCA Program from the Catalan Government (Generalitat de Catalunya). J.A. is a Serra Hünter Fellow (Generalitat de Catalunya). The project that gave rise to these results received the support of a fellowship (code is LCF/BQ/IN17/11620004) from la Caixa Foundation (identifier [ID] 100010434). This project has received funding from the European Union's Horizon 2020 research and innovation program under Marie Skłodowska-Curie grant agreement no. 713673.

We thank Joan Ruiz (Universitat Autònoma de Barcelona [UAB]) and Susana Escribano (UAB) for their excellent technical assistance, as well as UAB student Paula García for her helpful support.

M.V., J.A., N.S.C., and J.B. conceived the study. J.A. and J.C. performed the *in vitro* bacterial experiments. J.C. and P.S. performed all the bacterial infections *in planta*. M.V., J.A., N.S.C., and J.C. supervised the study. M.V., J.A., J.C., and P.S. analyzed the results. M.V., J.A., N.S.C., J.B., J.C., and P.S. wrote the article with contributions from all of us.

We declare that we have no conflict of interests.

REFERENCES

- Peeters N, Guidot A, Vaillau F, Valls M. 2013. *Ralstonia solanacearum*, a widespread bacterial plant pathogen in the post-genomic era. *Mol Plant Pathol* 14:651–662. <https://doi.org/10.1111/mpp.12038>.
- Allen C, Prior P, Hayward AC. 2005. Bacterial wilt disease and the *Ralstonia solanacearum* species complex. American Phytopathological Society Press, St. Paul, MN.
- Mansfield J, Genin S, Magori S, Citovsky V, Sriariyanum M, Ronald P, Dow M, Verdier V, Beer SV, Machado MA, Toth I, Salmond G, Foster GD. 2012. Top 10 plant pathogenic bacteria in molecular plant pathology. *Mol Plant Pathol* 13:614–629. <https://doi.org/10.1111/j.1364-3703.2012.00804.x>.
- Caldwell D, Kim B-S, Iyer-Pascuzzi AS. 2017. *Ralstonia solanacearum* differentially colonizes roots of resistant and susceptible tomato plants. *Phytopathology* 107:528–536. <https://doi.org/10.1094/PHYTO-09-16-0353-R>.
- Tans-Kersten J, Huang H, Allen C. 2001. *Ralstonia solanacearum* needs motility for invasive virulence on tomato. *J Bacteriol* 183:3597–3605. <https://doi.org/10.1128/JB.183.12.3597-3605.2001>.
- Yao J, Allen C. 2006. Chemotaxis is required for virulence and competitive fitness of the bacterial wilt pathogen *Ralstonia solanacearum*. *J Bacteriol* 188:3697–3708. <https://doi.org/10.1128/JB.188.10.3697-3708.2006>.
- Mattick JS. 2002. Type IV pili and twitching motility. *Annu Rev Microbiol* 56:289–314. <https://doi.org/10.1146/annurev.micro.56.012302.160938>.
- Kang Y, Liu H, Genin S, Schell MA, Denny TP. 2002. *Ralstonia solanacearum* requires type 4 pili to adhere to multiple surfaces and for natural transformation and virulence. *Mol Microbiol* 46:427–437. <https://doi.org/10.1046/j.1365-2958.2002.03187.x>.
- Liu H, Kang Y, Genin S, Schell MA, Denny TP, Genin S, Denny TP. 2001. Twitching motility of *Ralstonia solanacearum* requires a type IV pilus system. *Microbiology* 147:3215–3229. <https://doi.org/10.1099/00221287-147-12-3215>.
- Bertrand JJ, West JT, Engel JN. 2010. Genetic analysis of the regulation of type IV pilus function by the Chp chemosensory system of *Pseudomonas aeruginosa*. *J Bacteriol* 192:994–1010. <https://doi.org/10.1128/JB.01390-09>.
- Sampedro I, Parales RE, Krell T, Hill JE. 2015. *Pseudomonas* chemotaxis. *FEMS Microbiol Rev* 39:17–46. <https://doi.org/10.1111/1574-6976.12081>.
- Bahar O, Levi N, Burdman S, Burdman S. 2011. The cucurbit pathogenic bacterium *Acidovorax citrulli* requires a polar flagellum for full virulence before and after host-tissue penetration. *Mol Plant Microbe Interact* 24:1040–1050. <https://doi.org/10.1094/MPMI-02-11-0041>.
- Bahar O, Goffer T, Burdman S. 2009. Type IV pili are required for virulence, twitching motility, and biofilm formation of *Acidovorax avenae* subsp. *citrulli*. *Mol Plant Microbe Interact* 22:909–920. <https://doi.org/10.1094/MPMI-22-8-0909>.
- Taguchi F, Ichinose Y. 2011. Role of type IV pili in virulence of *Pseudomonas syringae* pv. *tabaci* 6605: correlation of motility, multidrug resistance, and HR-inducing activity on a nonhost plant. *Mol Plant Microbe Interact* 24:1001–1011. <https://doi.org/10.1094/MPMI-02-11-0026>.
- Monteiro F, Solé M, van Dijk I, Valls M. 2012. A chromosomal insertion toolbox for promoter probing, mutant complementation, and pathogenicity studies in *Ralstonia solanacearum*. *Mol Plant Microbe Interact* 25:557–568. <https://doi.org/10.1094/MPMI-07-11-0201>.
- Wheatley RM, Poole PS. 2018. Mechanisms of bacterial attachment to roots. *FEMS Microbiol Rev* 42:448–461. <https://doi.org/10.1093/femsre/fuy014>.
- Whitchurch CB, Leech AJ, Young MD, Kennedy D, Sargent JL, Bertrand JJ, Semmler ABT, Mellick AS, Martin PR, Alm RA, Hobbs M, Beatson SA, Huang B, Nguyen L, Commolli JC, Engel JN, Darzins A, Mattick JS. 2004. Characterization of a complex chemosensory signal transduction system which controls twitching motility in *Pseudomonas aeruginosa*. *Mol Microbiol* 52:873–893. <https://doi.org/10.1111/j.1365-2958.2004.04026.x>.
- Zhou X, Qian G, Chen Y, Du L, Liu F, Yuen GY. 2015. PilG is involved in the regulation of twitching motility and antifungal antibiotic biosynthesis in the biological control agent *Lysobacter enzymogenes*. *Phytopathology* 105:1318–1324. <https://doi.org/10.1094/PHYTO-12-14-0361-R>.
- Darzins A. 1994. Characterization of a *Pseudomonas aeruginosa* gene cluster involved in pilus biosynthesis and twitching motility: sequence similarity to the chemotaxis proteins of enterics and the gliding bacterium *Myxococcus xanthus*. *Mol Microbiol* 11:137–153. <https://doi.org/10.1111/j.1365-2958.1994.tb00296.x>.
- Cursino L, Galvani CD, Athinuwat D, Zaini PA, Li Y, De la Fuente L, Hoch HC, Burr TJ, Mowery P. 2011. Identification of an operon, Pil-Chp, that controls twitching motility and virulence in *Xylella fastidiosa*. *Mol Plant Microbe Interact* 24:1198–1206. <https://doi.org/10.1094/MPMI-10-10-0252>.
- Leech AJ, Mattick JS. 2006. Effect of site-specific mutations in different phosphotransfer domains of the chemosensory protein ChpA on *Pseudomonas aeruginosa* motility. *J Bacteriol* 188:8479–8486. <https://doi.org/10.1128/JB.00157-06>.
- Fulcher NB, Holliday PM, Klem E, Cann MJ, Wolfgang MC. 2010. The *Pseudomonas aeruginosa* Chp chemosensory system regulates intracellular cAMP levels by modulating adenylate cyclase activity. *Mol Microbiol* 76:889–904. <https://doi.org/10.1111/j.1365-2958.2010.07135.x>.
- Zhou M, Shen D, Xu G, Liu F, Qian G. 2017. ChpA controls twitching motility and broadly affects gene expression in the biological control agent *Lysobacter enzymogenes*. *Curr Microbiol* 74:566–574. <https://doi.org/10.1007/s00284-017-1202-5>.
- Rosenberg T, Salam BB, Burdman S. 2018. Association between loss of type IV pilus synthesis ability and phenotypic variation in the cucurbit pathogenic bacterium *Acidovorax citrulli*. *Mol Plant Microbe Interact* 31:548–559. <https://doi.org/10.1094/MPMI-12-17-0324-R>.
- Kilmury SLN, Burrows LL. 2018. The *Pseudomonas aeruginosa* PilSR two-component system regulates both twitching and swimming motilities. *mBio* 9:e01310-18. <https://doi.org/10.1128/mBio.01310-18>.
- Brumbley SM, Denny TP. 1990. Cloning of wild-type *Pseudomonas solanacearum* *phcA*, a gene that when mutated alters expression of multiple traits that contribute to virulence. *J Bacteriol* 172:5677–5685. <https://doi.org/10.1128/jb.172.10.5677-5685.1990>.
- Meng F, Yao J, Allen C. 2011. A MotN mutant of *Ralstonia solanacearum* is hypermotile and has reduced virulence. *J Bacteriol* 193:2477–2486. <https://doi.org/10.1128/JB.01360-10>.
- Das A, Rangaraj N, Sonti RV. 2009. Multiple adhesin-like functions of *Xanthomonas oryzae* pv. *oryzae* are involved in promoting leaf attachment, entry, and virulence on rice. *Mol Plant Microbe Interact* 22:73–85. <https://doi.org/10.1094/MPMI-22-1-0073>.
- Ryan RP, Fouhy Y, Lucey JF, Jiang B-L, He Y-Q, Feng J-X, Tang J-L, Dow JM. 2007. Cyclic di-GMP signalling in the virulence and environmental adaptation of *Xanthomonas campestris*. *Mol Microbiol* 63:429–442. <https://doi.org/10.1111/j.1365-2958.2006.05531.x>.
- Narulita E, Addy HS, Kawasaki T, Fujie M, Yamada T. 2016. The involvement of the PilQ secretin of type IV pili in phage infection in *Ralstonia solanacearum*. *Biochem Biophys Res Commun* 469:868–872. <https://doi.org/10.1016/j.bbrc.2015.12.071>.
- Siri MI, Sanabria A, Boucher C, Pianzola MJ. 2014. New type IV pili-related genes involved in early stages of *Ralstonia solanacearum* potato infection. *Mol Plant Microbe Interact* 27:712–724. <https://doi.org/10.1094/MPMI-07-13-0210-R>.
- Addy HS, Askora A, Kawasaki T, Fujie M, Yamada T. 2012. Through infection by φ RSM filamentous phages. *Phytopathology* 102:469–477. <https://doi.org/10.1094/PHYTO-11-11-0319-R>.
- Ray SK, Kumar R, Peeters N, Boucher C, Genin S. 24 March 2015, posting date. *rpoN1*, but not *rpoN2*, is required for twitching motility, natural competence, growth on nitrate, and virulence of *Ralstonia solanacearum*. *Front Microbiol* <https://doi.org/10.3389/fmicb.2015.00229>.
- McCarthy Y, Ryan RP, O'Donovan K, He Y-Q, Jiang B-L, Feng J-X, Tang J-L, Dow JM. 2008. The role of PilZ domain proteins in the virulence of

- Xanthomonas campestris* pv. *campestris*. *Mol Plant Pathol* 9:819–824. <https://doi.org/10.1111/j.1364-3703.2008.00495.x>.
35. Shi X, Lin H. 8 April 2016, posting date. Visualization of twitching motility and characterization of the role of the PilG in *Xylella fastidiosa*. *J Vis Exp* <https://doi.org/10.3791/53816>.
 36. Haiko J, Westerlund-Wikström B. 2013. The role of the bacterial flagellum in adhesion and virulence. *Biology (Basel)* 2:1242–1267. <https://doi.org/10.3390/biology2041242>.
 37. Rossi FA, Medeot DB, Liaudat JP, Pistorio M, Jofré E. 2016. In *Azospirillum brasilense*, mutations in *flmA* or *flmB* genes affect polar flagellum assembly, surface polysaccharides, and attachment to maize roots. *Microbiol Res* 190:55–62. <https://doi.org/10.1016/j.micres.2016.05.006>.
 38. Zheng H, Mao Y, Teng J, Zhu Q, Ling J, Zhong Z. 2015. Flagellar-dependent motility in *Mesorhizobium tianshanense* is involved in the early stage of plant host interaction: study of an *flgE* mutant. *Curr Microbiol* 70:219–227. <https://doi.org/10.1007/s00284-014-0701-x>.
 39. Mhedbi-Hajri N, Jacques M-A, Koebnik R. 2011. Adhesion mechanisms of plant-pathogenic *Xanthomonadaceae*. *Adv Exp Med Biol* 715:71–89. https://doi.org/10.1007/978-94-007-0940-9_5.
 40. Croes CL, Moens S, van Bastelaere E, Vanderleyden J, Michiels KW. 1993. The polar flagellum mediates *Azospirillum brasilense* adsorption to wheat roots. *J Gen Microbiol* 139:2261–2269. <https://doi.org/10.1099/00221287-139-9-2261>.
 41. Belas R. 2014. Biofilms, flagella, and mechanosensing of surfaces by bacteria. *Trends Microbiol* 22:517–527. <https://doi.org/10.1016/j.tim.2014.05.002>.
 42. O'Toole GA, Kolter R. 1998. Flagellar and twitching motility are necessary for *Pseudomonas aeruginosa* biofilm development. *Mol Microbiol* 30:295–304. <https://doi.org/10.1046/j.1365-2958.1998.01062.x>.
 43. Yao J, Allen C. 2007. The plant pathogen *Ralstonia solanacearum* needs aerotaxis for normal biofilm formation and interactions with its tomato host. *J Bacteriol* 189:6415–6424. <https://doi.org/10.1128/JB.00398-07>.
 44. Miller JH. 1972. Experiments in molecular genetics. Cold Spring Harbor Laboratory, Cold Spring Harbor, NY.
 45. Boucher CA, Barberis PA, Demery DA. 1985. Transposon mutagenesis of *Pseudomonas solanacearum*: isolation of Tn5-induced avirulent mutants. *Microbiology* 131:2449–2457. <https://doi.org/10.1099/00221287-131-9-2449>.
 46. Hendrick CA, Sequeira L. 1984. Lipopolysaccharide-defective mutants of the wilt pathogen *Pseudomonas solanacearum*. *Appl Environ Microbiol* 48:94–101. <https://doi.org/10.1128/AEM.48.1.94-101.1984>.
 47. Powell S, Forslund K, Szklarczyk D, Trachana K, Roth A, Huerta-Cepas J, Gabaldón T, Rattei T, Creevey C, Kuhn M, Jensen LJ, von Mering C, Bork P. 2014. eggNOG v4.0: nested orthology inference across 3686 organisms. *Nucleic Acids Res* 42:D231–D239. <https://doi.org/10.1093/nar/gkt1253>.
 48. Yu J-H, Hamari Z, Han K-H, Seo J-A, Reyes-Domínguez Y, Scazzocchio C. 2004. Double-joint PCR: a PCR-based molecular tool for gene manipulations in filamentous fungi. *Fungal Genet Biol* 41:973–981. <https://doi.org/10.1016/j.fgb.2004.08.001>.
 49. Monteiro F, Genin S, van Dijk I, Valls M. 2012. A luminescent reporter evidences active expression of *Ralstonia solanacearum* type III secretion system genes throughout plant infection. *Microbiology* 158:2107–2116. <https://doi.org/10.1099/mic.0.058610-0>.
 50. Raza W, Ling N, Yang L, Huang Q, Shen Q. 2016. Response of tomato wilt pathogen *Ralstonia solanacearum* to the volatile organic compounds produced by a biocontrol strain *Bacillus amyloliquefaciens* SQR-9. *Sci Rep* 6:24856. <https://doi.org/10.1038/srep24856>.
 51. Adler J. 1973. A method for measuring chemotaxis and use of the method to determine optimum conditions for chemotaxis by *Escherichia coli*. *J Gen Microbiol* 74:77–91. <https://doi.org/10.1099/00221287-74-1-77>.
 52. Bertolla F, Van Gijsegem F, Nesme X, Simonet P. 1997. Conditions for natural transformation of *Ralstonia solanacearum*. *Appl Environ Microbiol* 63:4965–4968. <https://doi.org/10.1128/AEM.63.12.4965-4968.1997>.
 53. Paola A, Cruz Z, Ferreira V, Pianzola MJ, Siri MI, Coll NS, Valls M. 2014. A novel, sensitive method to evaluate potato germplasm for bacterial wilt resistance using a luminescent *Ralstonia solanacearum* reporter strain. *Mol Plant Microbe Interact* 27:277–285. <https://doi.org/10.1094/MPMI-10-13-0303-FI>.
 54. O'Toole GA, Kolter R. 1998. Initiation of biofilm formation in *Pseudomonas fluorescens* WCS365 proceeds via multiple, convergent signalling pathways: a genetic analysis. *Mol Microbiol* 28:449–461. <https://doi.org/10.1046/j.1365-2958.1998.00797.x>.
 55. Yang W-C, Lin Y-M, Cheng Y-S, Cheng C-P. 2013. *Ralstonia solanacearum* *RSc0411* (*lptC*) is a determinant for full virulence and has a strain-specific novel function in the T3SS activity. *Microbiology* 159:1136–1148. <https://doi.org/10.1099/mic.0.064915-0>.
 56. Morel A, Peeters N, Vailliau F, Barberis P, Jiang G, Berthomé R, Guidot A. 2018. Plant pathogenicity phenotyping of *Ralstonia solanacearum* strains. *Methods Mol Biol* 1734:223–239. https://doi.org/10.1007/978-1-4939-7604-1_18.
 57. Puigvert M, Solé M, López-García B, Coll NS, Beattie KD, Davis RA, Elofsson M, Valls M. 2019. Type III secretion inhibitors for the management of bacterial plant diseases. *Mol Plant Pathol* 20:20–32. <https://doi.org/10.1111/mpp.12736>.